






Magnetic Connectivity between the Light Bridge and Penumbra in a Sunspot

Song Feng^{1,2} , Yuhu Miao³, Ding Yuan³ , Zhongquan Qu², and Valery M. Nakariakov^{4,5} 

¹ Yunnan Key Laboratory of Computer Technology Application, Faculty of Information Engineering and Automation, Kunming University of Science and Technology, Kunming 650500, People's Republic of China

² Yunnan Astronomical Observatory, Chinese Academy of Sciences, P.O. Box 110, Kunming 650011, People's Republic of China

³ Institute of Space Science and Applied Technology, Harbin Institute of Technology, Shenzhen, Guangdong 518055, People's Republic of China; yuanding@hit.edu.cn

⁴ Centre for Fusion, Space and Astrophysics, Department of Physics, University of Warwick, CV4 7AL, UK

⁵ St. Petersburg Branch, Special Astrophysical Observatory, Russian Academy of Sciences, St. Petersburg, 196140, Russia

Received 2019 December 31; revised 2020 March 6; accepted 2020 March 8; published 2020 April 7

Abstract

A light bridge is a prominent structure commonly observed within a sunspot. Its presence usually triggers a wealth of dynamics in a sunspot and has a lasting impact on sunspot evolution. However, the fundamental structure of light bridges is still not well understood. In this study, we used the high-resolution spectropolarimetry data obtained by the Solar Optical Telescope on board the Hinode satellite to analyze the magnetic and thermal structure of a light bridge at AR 12838. We also combined the high-cadence 1700 Å channel data provided by the Atmospheric Imaging Assembly on board the Solar Dynamics Observatory to study the dynamics on this bridge. We found a pair of blue and red Doppler shift patches at two ends of this bridge; this pattern appears to be the convective motion directed by the horizontal component of the magnetic field aligned with the spine of the bridge. Paired upward and downward motions imply that the light bridge could have a two-legged or undulating magnetic field. Significant 4 minute oscillations in the emission intensity of the 1700 Å bandpass were detected at two ends, which overlapped the paired blue- and redshift patches. The oscillatory signals at the light bridge and the penumbra were highly correlated with each other. Although they are separated in space at the photosphere, the periodicity seems to have a common origin from underneath the sunspot. Therefore, we infer that the light bridge and penumbra could share a common magnetic source and become fragmented at the photosphere by magnetoconvection.

Unified Astronomy Thesaurus concepts: [Sunspots \(1653\)](#); [Magnetohydrodynamics \(1964\)](#); [Sunspot flow \(1978\)](#); [Solar coronal waves \(1995\)](#); [Solar magnetic fields \(1503\)](#); [Solar magnetic reconnection \(1504\)](#)

1. Introduction

A light bridge is an elongated bright structure that either crosses a sunspot umbra or deeply penetrates it (Muller 1979). This type of structure is usually found in a nascent or decaying spot, or when two spots merge into one or the inverse process occurs. At these stages, magnetoconvection causes significant flux separation in deeper layers of a spot or pore, and this phenomenon could be accompanied by the formation of light bridges and umbral dots at the photosphere (Bharti et al. 2007a; Rempel 2011; Toriumi et al. 2015a). Light bridges could affect the evolution of sunspots, e.g., causing them to split or merge; they consequently determine the level of solar activities indirectly.

According to Sobotka (1997), a light bridge is classified either as a granular bridge if it exhibits photospheric dynamics, or a filamentary bridge if it is an intrusion of penumbra. For further classification it is termed either as a strong light bridge if it separates the umbra, or as a faint light bridge if it simply protrudes into the umbra. In the following text, we use “spine” to refer to the elongated central column of a light bridge. The two “ends” are a bridge’s shorter edges, which normally have a length of a few arcseconds, and the two “flanks” are the longer edges, which usually have length scales comparable to the umbra.

A light bridge is believed to be hotter than the umbra, as convection (granulations) is partially or fully restored therein (Roupe van der Voort et al. 2010). Convection could act as an effective mechanism to supply hotter gas to the light bridge.

Hot and dense plasma is pushed upwards at the spine of a bridge and moves downwards at its two flanks (Lagg et al. 2014). Strong downflow would drag the magnetic field lines and could even lead to polarity reversal in extreme cases (Bharti et al. 2007b).

The magnetic field of a light bridge is more inclined than the vertical umbral field, and a magnetic canopy model is proposed for a light bridge (Jurčák et al. 2006). Strong discontinuity is found at the interface between a light bridge and the umbra; therefore, strong electric current density could be detected at the edge of a bridge (Shimizu 2011; Toriumi et al. 2015a, 2015b).

Many dynamic activities are detected at light bridges, as a light bridge has a magnetic and thermal structure in contrast with that of the umbra. Louis et al. (2014) found that dynamic jets usually originate from one flank of a bridge and propagate along the open magnetic field lines. According to the asymmetry in jet excitation, Yuan & Walsh (2016) proposed a three-dimensional model for a light bridge: the magnetic field at one flank is mostly aligned with umbral field, whereas at the other flank the two magnetic fields are closer to antiparallel. In this scenario, magnetic reconnections, which are believed to be the drivers of jets (Moore et al. 2010), could only be triggered at one flank.

Robustini et al. (2016) and Tian et al. (2018) detected inverted Y-shaped jets above sunspot light bridges, this morphology supports the model of flux emergence in the vertical umbral magnetic field, the collimated jets and surges are propelled by the reconnections between antiparallel

magnetic field lines. These kinds of activities are also reported by a number of studies (Bharti et al. 2017; Bai et al. 2019).

A sunspot is usually a host of waves and oscillations. In the umbra, the oscillation period is about three minutes, whereas in the penumbra, a dominant oscillation could be found at the five minute bandpass (Khomenko & Collados 2015). Above a light bridge, five minute oscillations similar to penumbra oscillations are usually detected; however, their origin is still not revealed (Yuan et al. 2014; Yang et al. 2015; Yuan & Walsh 2016).

In this study, a tiny light bridge is formed in the center of the umbra, and the ambient magnetic field is very simple. This situation hence allows for a decent investigation of light bridge properties with negligible contamination of other structures. In Section 2, we presents data reduction and analysis. Then we cover the structure and dynamics on this light bridge in Section 3. In Section 4, we discuss the possible structure of a light bridge with the knowledge obtained in this study.

2. Data Reduction and Analysis

On 2019 April 10 and 11, a penumbral filament protruded into the umbra of AR 12838 and formed a faint light bridge (see Figure 1). This light bridge detached from the penumbral filament and evolved into a compact and isolated structure on April 12 and 13. From April 14 and thereafter, the light bridge became more diffuse and eventually decayed. This light bridge was clearly visible in the 1700 Å, 1600 Å, and visible light (4500 Å) channels of the Atmospheric Imaging Assembly (AIA; Lemen et al. 2012) on board the Solar Dynamics Observatory (SDO) from 2019 April 10 to 15.

SDO/AIA observes the full solar disk continuously with nine filters in ultra violet (UV) and extreme UV (EUV) bandpasses. One AIA pixel corresponds to an angular width of 0".6 or a distance of about 435 km on the Sun. The UV channels take an image of the Sun every 24 s, whereas the EUV images have a cadence of about 12 s.

The Helioseismic and Magnetic Imager (HMI) on board SDO observes the full solar disk at 6173 Å, one pixel corresponds to 0".5. The line-of-sight magnetogram has a cadence of about 45 s.

The AIA UV and EUV data were calibrated with the standard procedure provided by SolarSoft.⁶ The digital offset of the cameras, CCD read-out noise, and dark current were removed from the data, then each image was corrected with a flat field and was normalized with its exposure time.

The spectropolarimeter (SP) of the Solar Optical Telescope (SOT) on board the Hinode mission measured high-precision Stokes polarimetric line profiles of the FeI 6301.5 Å and 6302.5 Å spectral lines. The fast-mapping mode was used to scan the entire sunspot and its surrounding area. Each pixel represented an angular width of about 0".32; the spectral sampling was about 21.549 mÅ per pixel. Two consecutive slit scans had a step size of about 0".30.

We obtained SOT/SP level-2 data from Community Spectro-polarimetric Analysis Center (CSAC⁷). This data set has undergone the standard CCD image calibration. The Stokes parameters were used to derive the magnetic field vector and flow field by assuming the Milne-Eddington Atmosphere model (see the review by del Toro Iniesta & Ruiz Cobo 2016). The 180° ambiguity of the azimuth angle of the magnetic field

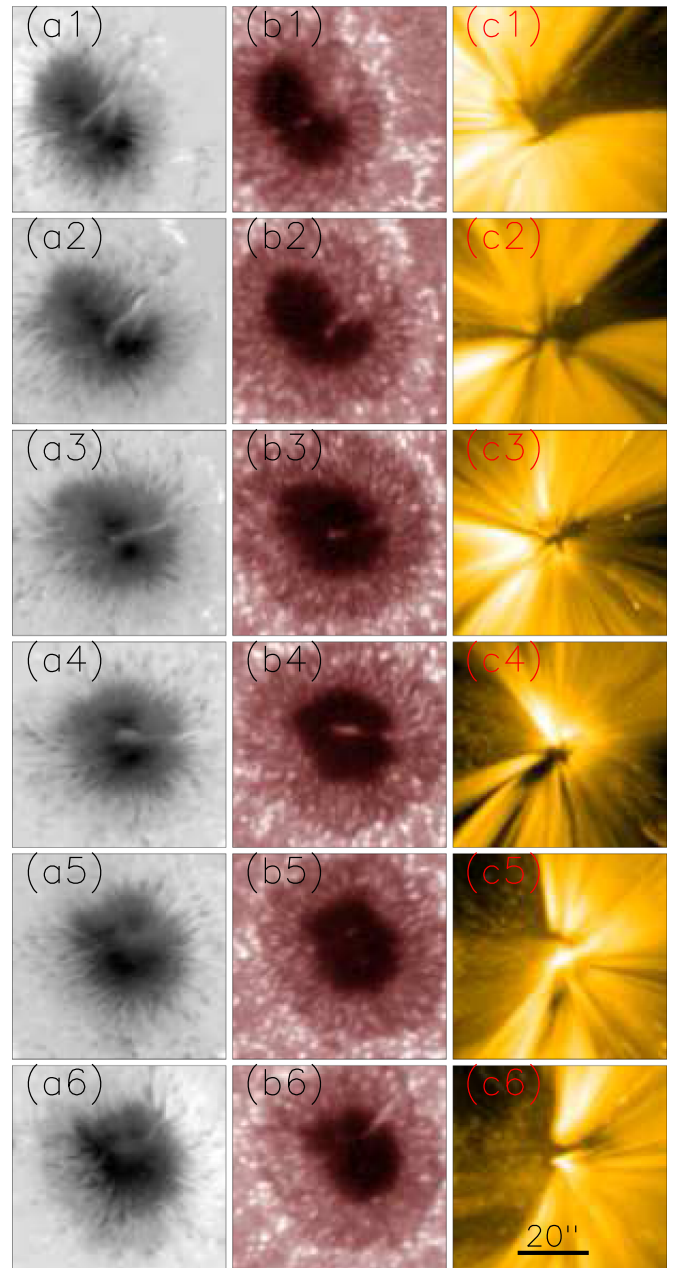


Figure 1. Evolution of the sunspot and diffuse coronal loops associated with active region 12738. The left (a), middle (b), and right (c) columns draw the images of HMI LOS magnetogram, AIA 1700 Å, and AIA 171 Å channels, respectively. Numbers 1–6 denote the observations at about 10:00 UT on consecutive dates from 2019 April 10 to 2019 April 15.

was resolved with the AZAM utility (Lites et al. 1995). The SP images were aligned with the AIA UV images by matching the center of the light bridge. The vertical electric current density (j_z) was computed by using the inverted vector magnetic field, $j_z = \mu_0^{-1}(\nabla \times \mathbf{B})_z$, where μ_0 stands for the magnetic permeability in free space. The Doppler shift was obtained by the inversion of the Stokes vector.

We extracted the emission intensity variations of the 1700 Å channel from a pixel in the umbra and another one at the light bridge (Figure 2(d)). These two time series were detrended by removing the 10 minute moving average; the wavelet spectra were calculated with the Morlet mother function (Torrence & Compo 1998). The detrended emission intensity variations and

⁶ http://www.lmsal.com/solarsoft/ssw_install.html

⁷ https://csac.hao.ucar.edu/sp_data.php

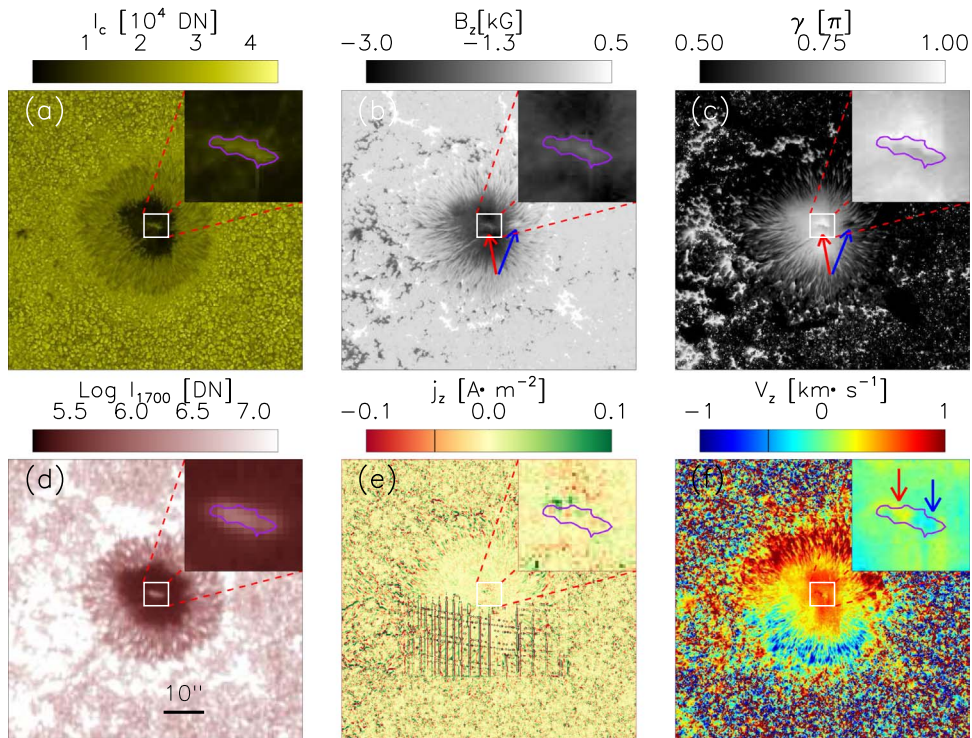


Figure 2. Maps of the SOT/SP continuum intensity at $\lambda 6301.5 \text{ \AA}$ (a), the LOS magnetic field component (b), the inclination angle of magnetic field vector (c), the electric current density (e), the Doppler shift velocity (f), and the emission intensity of the AIA 1700 Å channel (d). The top-right window of each panel highlights the zoomed-in view of the light bridge. A pair of red and blue arrows highlight the light bridge and another region with mixed polarity at the penumbra. In the zoomed-in window of (f), the local background velocity has been removed to highlight the Doppler shift above the light bridge.

wavelet spectra are plotted in Figure 3 for both cases of light bridge and umbra. We see that an oscillatory signal with a period of about two minutes was detected in the umbra (Figure 3(b)), whereas the light bridge exhibited a four minute oscillation (Figure 3(d)).

To study the spatial distribution of four minute oscillations, we performed Fourier transform on the detrended emission intensity of every pixel in AIA 1700 Å and averaged the Fourier power among the spectral components between three and five minutes. Figure 4(a) plots the narrowband Fourier power with four minute spectral peak above 3σ noise level. The noise level was estimated by assuming the white noise in the times series as formulated in Torrence & Compo (1998).

We also analyzed the correlation between the four minute oscillations at the light bridge and those at the penumbra. For every pixel, the detrended emission intensity was transformed into the Fourier space, then a narrowband spectrum was selected by multiplying a uniform window between three to five minutes. Thereafter, a filtered signal in the time domain was formed by doing inverse Fourier transform. A reference signal was estimated by averaging the signals within the light bridge (within the island as enclosed by the inner contour in Figure 4). We calculated the cross-correlation between the signal of every pixel and the reference signal; the maximum cross-correlation coefficient and lag time for each pixel were obtained by finding the argument maximum. These two values were plotted in Figures 4(b)–(c).

A similar analysis was done for the two minute bandpass (the two to three minute range). The Fourier power, cross-correlation coefficient, and lag time distributions are shown in Figures 4(d)–(f).

3. Structure and Dynamics of the Light Bridge

3.1. Suppression of Coronal Loop Formation

Figure 1 presents the evolution of this sunspot and the associated active region AR 12838 with expanding coronal loops. An interesting feature is that on 2019 April 10 and 11. This light bridge was anchored at the northwest part of the penumbra (Figures 1(a1)–(a2)), and no coronal loops were rooted at that part (Figures 1(c1)–(c2)). In contrast to this, after the bridge gradually detached from the penumbra, the coronal loops started to form again (Figures 1(c4)–(c6)). It appears that such a light bridge suppressed the formation of coronal loops above the part of the umbra where it has rooted. We noted that at the region where the light bridge was rooted, the strength and inclination angle of the magnetic field deviated from the other part of the penumbra (Figures 2(b)–(c)). This part seems to have mixed polarity in contrast to the negative polarity at the umbra (see the part pointed out by a blue arrow in Figure 2(b)).

3.2. Thermal and Magnetic Structure

In this section and thereafter, we focus on the compact and segmented light bridge on 2019 April 13 (Figure 1(b4)). This structure could stand clear of the influence of complex dynamics, as its size was small and its magnetic structure might reveal the fundamental structure of a light bridge.

Figure 2 illustrates the structure of the magnetic field and Doppler shift obtained by inversion of the SOT/SP Stokes vector. We could see that, in the continuum intensity at $\lambda 6301.5 \text{ \AA}$ and the emission intensity of AIA 1700 Å, the elementary light bridge formed a compact bright island within the umbra core (Figures 2(a) and (d)). Its LOS magnetic field component B_z was as weak as -1400 G , about half the strength

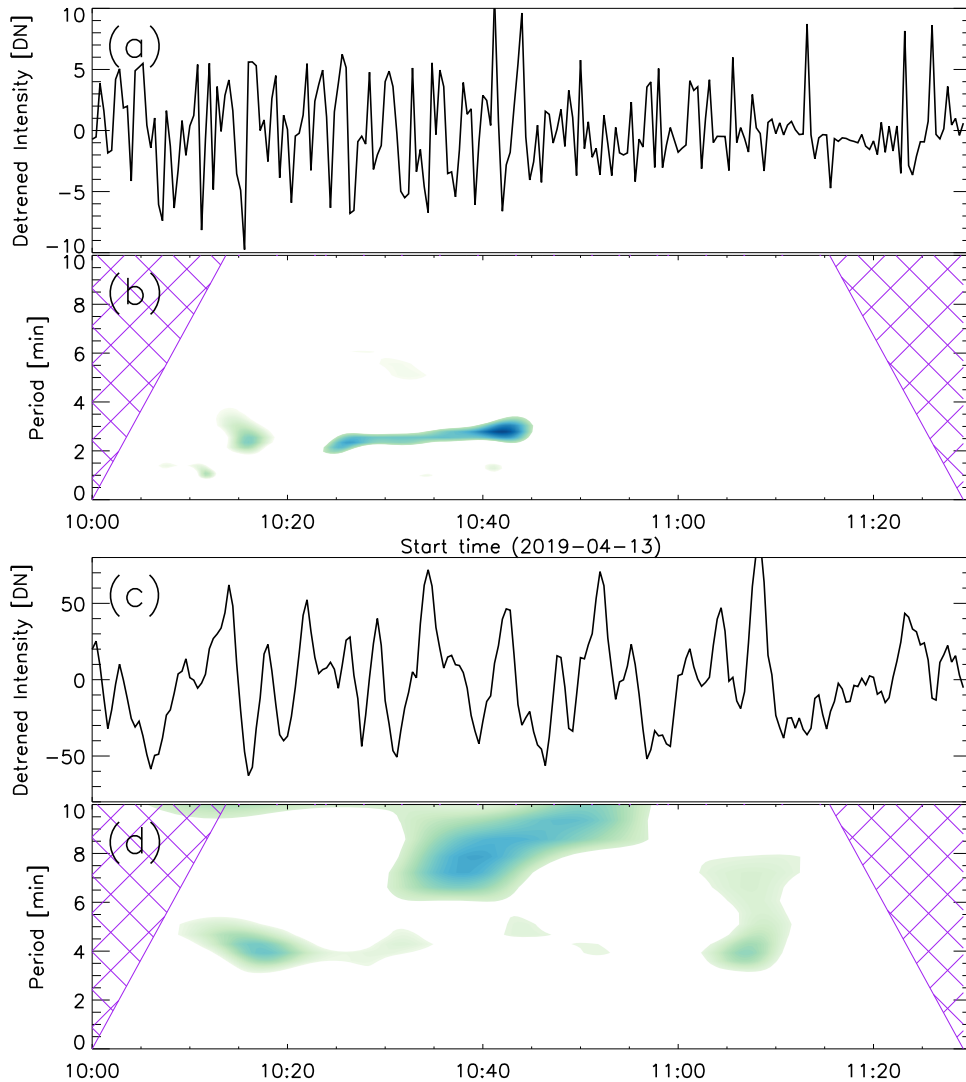


Figure 3. (a) Emission intensity of the AIA 1700 Å channel at a pixel on the umbra, 10 minute running averages were removed. (b) Wavelet power spectrum of the detrended signal. The reliable regions subject to the zero-padding effect are cross-hatched. (c)–(d) Same analysis done to a pixel on the light bridge.

of the umbral field (about -3000 G). This variation was very sharp (about 1500 G) and this was detected within a span of about $3''$ (or about 2000 km) across the bridge (Figure 2(b)). Along the elongated spine of the bridge, the variation of the LOS magnetic component was much smaller (about 500 G). This fact also holds in the inclination angle of the magnetic field vector: along the spine, the inclination angle did not vary significantly, whereas across the spine we could discern that inclination angle at two flanks deviated by about 30 deg (or about 0.15π , see Figure 2(c)). The electric current density was strong at the northern end of the bridge, but no clear pattern was discernible.

In Figure 2(f), we observed redshift at the northern penumbra, its magnitude was about 1 km s^{-1} . This means that fluid moved downwards to the sunspot. The Doppler shift was about 1 km s^{-1} at the outer edge of the penumbra, this value was stronger than that at the penumbra–umbra interface. This is a clear pattern of Evershed flow (Evershed 1909), which could be caused by overturning magnetoconvective motion guided by the magnetic field lines (Rimmele & Marino 2006; Siu-Tapia et al. 2018). The umbra was also overwhelmed by redshift; at the bridge, there were two regions with flows either stronger or

weaker than the background redshift. After removing the background redshift (about 0.6 km s^{-1}), we observed paired patches of red- and blueshifts on the western and eastern ends of this light bridge (Figure 2(f), zoomed view), their velocities were about ± 0.3 km s^{-1} .

3.3. Oscillations

Within the umbral core, we could see that the emission intensity exhibited a persistent oscillatory signal at about two minutes, see Figure 3. This oscillatory signal could be found within the whole umbra core, this is consistent with previous studies (Yuan et al. 2014; Jess et al. 2016; Yuan & Walsh 2016). The umbral oscillation power at two minutes became depleted at the light bridge. The cross-correlation of the two minute band was very low within the umbra (Figures 4(e) and (f)).

At the light bridge, the emission intensity varied periodically at about four minutes (Figure 3). This four minute signal filled the light bridge (Figure 4(a)). This is consistent with earlier studies (Yuan et al. 2014). Two patches of strong oscillation power were measured at two ends of the bridge. This pattern overlapped with the paired regions with red and blue Doppler

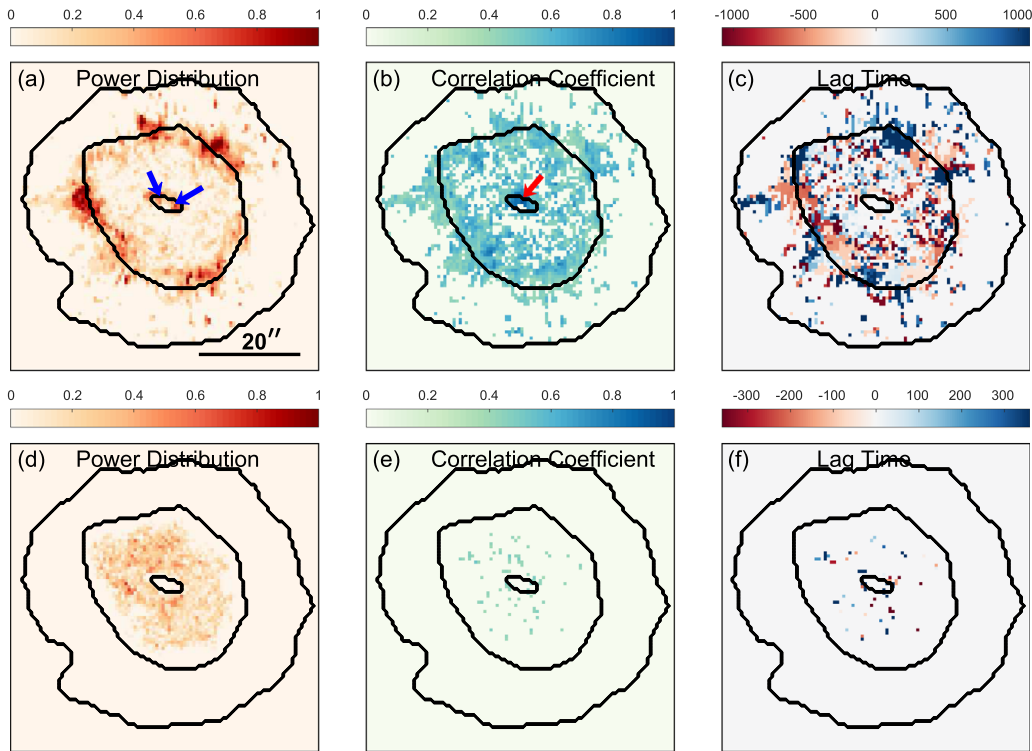


Figure 4. (a) Fourier power averaged over a 3–5 minute period range in the AIA 1700 Å channel. (b)–(c) The maximum cross-correlation coefficient and lag time for the time series filtered at the same bandpass. (d)–(f) The counterpart for the 1–3 minute period range.

shift. Within the bridge, the cross-correlation was very strong, the high-correlation region was found over the whole bridge (Figure 4(b)). The lag time of the four minute oscillation was close to zero within the bridge (Figure 4(c)).

At the penumbra, similar four minute oscillations were detected. The strong oscillation power was found to be distributed along the umbra-penumbra border. This is a commonly observed feature in sunspots (Yuan et al. 2014; Yuan & Walsh 2016). This oscillatory signal was separate in space from the light bridge oscillation (Figure 4(a)). However, we notice that the four minute oscillations at the penumbra and the light bridge had strong correlation (Figure 4(b)). In contrast, the two minute umbral oscillations had very weak correlation between any two locations (Figure 4(e)). The lag time at the penumbra could be either positive or negative, regions with the same lag time tended to form patches in sizes of a few arcseconds (Figure 4(c)), which means that the four minute oscillation within the same patch could originate from a common oscillatory source from underneath the sunspot.

4. Conclusions and Discussions

In this Letter, we used the joint observations of SDO/AIA and Hinode/SOT on AR 12838, and studied the long-term evolution of a light bridge, its magnetic and thermal structures, and the oscillations of emission intensity. With a wealth of observables, we aim to infer the origin and structure of this light bridge.

The light bridge appears to suppress the formation of coronal loops at the region where it is connected to the penumbra. The region rooted by the light bridge has mixed polarity in contrast to the umbral field, which means that the umbral field could connect to this polarity, rather than expand radially and form coronal loops.

On 2019 April 13, this bridge detached from the penumbra. A pair of red- and blueshifted regions were found at its two ends; whereas this whole structure was submerged within a global redshift. The paired patches of blue- and redshift indicated upward and downward motion of plasma along the line of sight. The radiative MHD simulations of Rempel (2011) and Toriumi et al. (2015a) suggest that magnetoconvections could be guided by strong inclined magnetic field and plays a key role in triggering the dynamics above the light bridge. The paired patches of blue and red Doppler shifts detected in this study imply that this light bridge has a strong horizontal magnetic field component along its spine and directed the magnetoconvection motions along its elongated part. This effect has also been observed in cool loops (Bethge et al. 2012), emerging magnetic flux tube (Requerey et al. 2017), and sunspot umbra (Kleint & Dalda 2013; Guglielmino et al. 2017, 2019).




Within the umbra of AR 12838 in this study, the emission intensity oscillates with a period of about two minutes; however, this oscillatory signal disappeared above the light bridge. In contrast, this light bridge was a host of four minute oscillation in the emission intensity. Moreover, this periodicity is commonly found at the penumbra. So it appears that the four minute oscillation at the light bridge and that at the penumbra has a common origin, as they were highly correlated. If a light bridge is transported to the surface by magnetoconvection (Toriumi et al. 2015a), its magnetic field could converge with that of the penumbra at a certain depth underneath the sunspot. That region could be the source of the four minute periodicity.

Here, we summarize the knowledge obtained within this Letter. A pair of blue- and redshift regions indicates that two ends of this light bridge are connected by a strong horizontal field. The paired upward and downward motions imply that this light bridge has a two-legged or undulating magnetic field. If

one end of this light bridge is rooted at the penumbra, it would suppress the formation of a coronal loop at the anchor region. The four minute oscillation at the light bridge is highly correlated with that at the penumbra; it indicates that the light bridge and penumbra structure could be connected at a certain depth under the surface, and they could have the same origin of a subsurface magnetic field flux and become fragmented by magnetoconvective motions (Rempel 2011; Toriumi et al. 2015a). With the flow pattern and oscillations, we could gain an insight into the internal structure and formation of a light bridge, we should note that this light bridge only represents one kind. More cases are needed to probe the general structure of light bridges and investigate their influence on the dynamics and evolution of sunspots and pores.

D.Y. is supported by the National Natural Science Foundation of China (NSFC, 11803005, 11911530690), Shenzhen Technology Project (JCYJ20180306172239618). S.F. is supported by the Joint Fund of NSFC (U1931107) and the Key Applied Basic Research program of the Yunnan Province (2018FA035). Wavelet software was provided by C. Torrence and G. Compo, and is available at <http://atoc.colorado.edu/research/wavelets/>.

ORCID iDs

Song Feng  <https://orcid.org/0000-0003-4709-7818>
 Ding Yuan  <https://orcid.org/0000-0002-9514-6402>
 Valery M. Nakariakov  <https://orcid.org/0000-0001-6423-8286>

References

Bai, X., Socas-Navarro, H., Nóbrega-Siverio, D., et al. 2019, *ApJ*, 870, 90
 Bethge, C., Beck, C., Peter, H., & Lagg, A. 2012, *A&A*, 537, A130

Bharti, L., Jain, R., & Jaaffrey, S. N. A. 2007a, *ApJL*, 665, L79
 Bharti, L., Rimmele, T., Jain, R., Jaaffrey, S. N. A., & Smartt, R. N. 2007b, *MNRAS*, 376, 1291
 Bharti, L., Solanki, S. K., & Hirzberger, J. 2017, *A&A*, 597, A127
 del Toro Iniesta, J. C., & Ruiz Cobo, B. 2016, *LRSP*, 13, 4
 Evershed, J. 1909, *MNRAS*, 69, 454
 Guglielmino, S. L., Romano, P., Cobo, B. R., Zuccarello, F., & Murabito, M. 2019, *ApJ*, 880, 34
 Guglielmino, S. L., Romano, P., & Zuccarello, F. 2017, *ApJL*, 846, L16
 Jess, D. B., Reznikova, V. E., Ryans, R. S. I., et al. 2016, *NatPh*, 12, 179
 Jurčák, J., Martínez Pillet, V., & Sobotka, M. 2006, *A&A*, 453, 1079
 Khomenko, E., & Collados, M. 2015, *LRSP*, 12, 6
 Kleint, L., & Dalda, A. S. 2013, *ApJ*, 770, 74
 Lagg, A., Solanki, S. K., van Noort, M., & Danilovic, S. 2014, *A&A*, 568, A60
 Lemen, J. R., Title, A. M., Akin, D. J., et al. 2012, *SoPh*, 275, 17
 Lites, B. W., Low, B. C., Martínez Pillet, V., et al. 1995, *ApJ*, 446, 877
 Louis, R. E., Beck, C., & Ichimoto, K. 2014, *A&A*, 567, A96
 Moore, R. L., Cirtain, J. W., Sterling, A. C., & Falconer, D. A. 2010, *ApJ*, 720, 757
 Muller, R. 1979, *SoPh*, 61, 297
 Rempel, M. 2011, *ApJ*, 740, 15
 Requerey, I. S., Ruiz Cobo, B., Del Toro Iniesta, J. C., et al. 2017, *ApJS*, 229, 15
 Rimmele, T., & Marino, J. 2006, *ApJ*, 646, 593
 Robustini, C., Leenaarts, J., de la Cruz Rodríguez, J., & Rouppe van der Voort, L. 2016, *A&A*, 590, A57
 Rouppe van der Voort, L., Bellot Rubio, L. R., & Ortiz, A. 2010, *ApJL*, 718, L78
 Shimizu, T. 2011, *ApJ*, 738, 83
 Siu-Tapia, A. L., Rempel, M., Lagg, A., & Solanki, S. K. 2018, *ApJ*, 852, 66
 Sobotka, M. 1997, in ASP Conf. Ser. 118, 1st Advances in Solar Physics Euroconference. Advances in Physics of Sunspots, ed. B. Schmieder, J. C. del Toro Iniesta, & M. Vázquez (San Francisco, CA: ASP), 155
 Tian, H., Yurchyshyn, V., Peter, H., et al. 2018, *ApJ*, 854, 92
 Toriumi, S., Cheung, M. C. M., & Katsukawa, Y. 2015a, *ApJ*, 811, 138
 Toriumi, S., Katsukawa, Y., & Cheung, M. C. M. 2015b, *ApJ*, 811, 137
 Torrence, C., & Compo, G. P. 1998, *BAMS*, 79, 61
 Yang, S., Zhang, J., Jiang, F., & Xiang, Y. 2015, *ApJL*, 804, L27
 Yuan, D., Nakariakov, V. M., Huang, Z., et al. 2014, *ApJ*, 792, 41
 Yuan, D., & Walsh, R. W. 2016, *A&A*, 594, A101